Macromolecules

pubs.acs.org/Macromolecules Article

Potential Universal Extensional Rheology in Concentrated Polymeric Liquids

Nuofei Jiang*

Cite This: *Macromolecules* 2024, 57, 5520−5532 Read Online

ACCESS | Metrics & More | Article Recommendations | Supporting Information

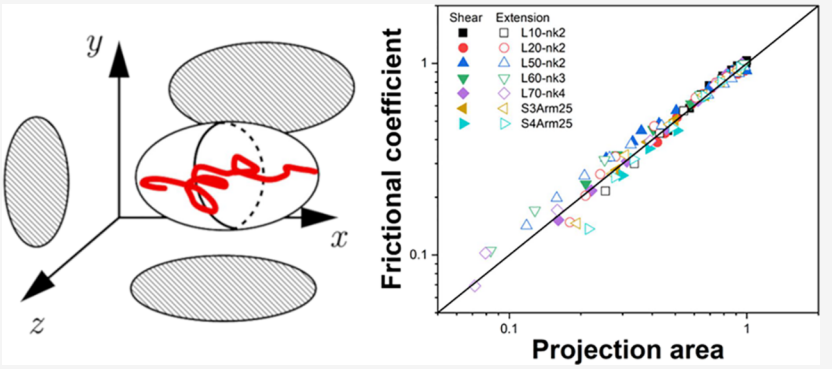

ABSTRACT: Polymer dynamics are special, in that they are always insensitive to the chemical details of the monomers. However, recent experiments show that the nonlinear extensional rheology of concentrated polymeric liquids has a nonuniversal feature. In this work, the variation of segmental frictional coefficient under flows, which is thought to be the critical factor in explaining the observed nonuniversality, is investigated in the coarse-grained (CG) molecular dynamics (MD) simulations of polymer melts. The frictional coefficients in the simulations are quantified from the expressions we proposed very recently [Jiang, N.; van Ruymbeke, E., *Macromolecules* **2023**, *56* (8), 2911−2929], which are based on the analytical relationships between the frictional coefficients and the observable rheological and structural properties. After the validation of the simulations with experimental data and our expressions, it is shown that those frictional coefficients can be universally related to the projection areas of the polymer coils in the plane normal to the direction of elongation. Moreover, this projection−friction relationship indicates a Kuhn-scale criterion of extensional viscosity, which suggests that a similar extensional rheology will be observed when the materials have the same number of Kuhn segments per chain N_k and the same reduced Kuhn density n_k defined as the ratio of the Kuhn length to the packing length. This criterion is tested on a series of new simulation systems designed to show similar steady-state extensional viscosities as a function of the reduced extensional rate, as well as the existing experimental data in the literature. The results of this work provide a helpful guideline in searching for the potential universal extensional rheology in the experimental samples.

1. INTRODUCTION

The dynamics of polymeric liquids differ significantly from the dynamics of small-molecule liquids, in that they are much more universal. The term "universal" means that different polymer species can have very similar dynamic behaviors, e.g., the frequency-dependent complex moduli can be superposed by means of vertical and horizontal shifts, given the proper molar mass and/or concentration of the samples. This idea is illustrated at the beginning of the textbook by Doi and Edwards:[1] The solutions of two chemically different polymers, one of which consists of spherical objects and the other has triangle-shaped segments, will have a similar macroscopic behavior as the large-scale properties of the polymer chain like the number of repeating units is the dominant factor. However, if the objects are no longer connected, the shape of the object will make a difference. For the melts or concentrated solutions of polymers, where the polymer chains are highly interpenetrated, universal dynamics are featured by both chain connectivity and the magnitude of interpenetration. For example, the tube model describes the motion of a long chain in the melt as reptation with a chemistry-dependent tube diameter.[1] At the same time, the Lin−Noolandi theory proposes that a cube with the edge length equal to the tube diameter can be filled by a fixed number of entanglement strands irrespective of the species,[2,3] which is supported by the extensive experimental data set shown by Fetters et al.[4] For short-chain systems without the entanglement

Received: December 26, 2023
Revised: May 3, 2024
Accepted: May 10, 2024
Published: May 22, 2024

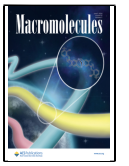

https://doi.org/10.1021/acs.macromol.3c02648
Macromolecules 2024, 57, 5520−5532

effect, it is found that the surrounding chains behave like a homogeneous viscous medium. In this case, the polymer dynamics can be well described by the very simple bead−spring chain (BSC) model, also called the Rouse model.[5] As a slight extension of Doi and Edwards's demonstration, we can design two polymer melts of the same chain length and magnitude of overlapping but composed of segments of different shapes, as shown in Figure 1a. Evidently, they will follow similar

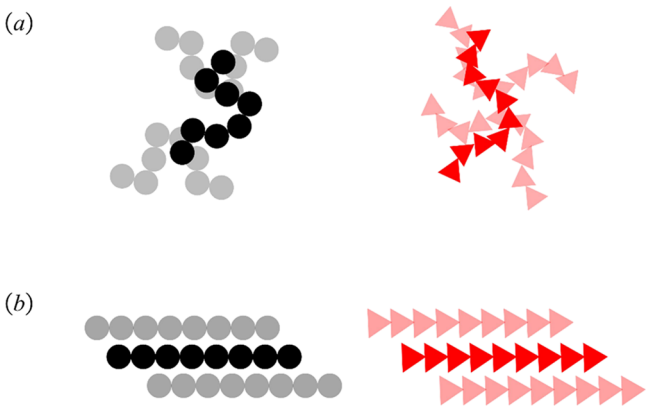

Figure 1. Two polymer melts composed of segments of different shapes in (a) equilibrium state and (b) nonequilibrium state.

macroscopic dynamics under equilibrium. In this sense, the chemical information about the monomers is described by the properties in terms of the Kuhn segment, including the Kuhn length, the packing length, and the frictional coefficient of the Kuhn segment. The universal feature of polymer dynamics has been widely confirmed from experimental facts for the linear viscoelastic (LVE) properties and is thought to be fundamental to the theory of polymer dynamics.[1]

The response to a constant and homogeneous extensional flow is one of the most fundamental dynamic properties of polymers. However, the experimental measurement covering the start-up of the flow and the steady state is very challenging to achieve in a concentrated polymeric liquid. With the development of experimental methodologies, especially since the appearance of the filament stretching rheometer,[6−8] the extensional rheology of melts or concentrated solutions of polymers can now be characterized with high accuracy. A large amount of experimental data have become available. At the same time, the existence of universal behavior in the nonlinear extensional rheology is questioned.[9] In a series of works by Huang, Hassager, and their co-workers,[10−13] they systematically compared the solutions and melts of polystyrene (PS) with the same number of entanglements. It was found that, while the two groups of samples have the same (normalized) LVE and nonlinear shear rheology, their responses to the extensional flows are significantly different. The steady-state extensional viscosity of the entangled PS melt only shows a strain-rate-thinning behavior, while in the solution of the same entanglement number, the extensional viscosity experiences thinning followed by thickening. That means more molecular information must be included to prepare the materials of similar extensional rheology. In a later work by Morelly et al.,[14] it was confirmed that the finite extensibility of the entanglement strand is also an essential factor to consider. Although the idea of identifying chemistry-independent properties under extension is appealing, it was nearly announced to be impossible after the experimental work by Matsumiya et al.,[15] who measured the extensional viscosities of the unentangled melts of PS and poly(p-*tert*-butylstyrene) (PtBS) with a similar number of Kuhn segments per chain (similar finite extensibility). It was found that even if their monomers' chemical structures are very similar, the two polymer melts behave very differently under extensional flows. This feature was reconfirmed in a recent work by Wu et al.[16] In that work, the authors synthesized a series of poly(*n*-alkyl methacrylate) samples with different lengths of the alkyl group. Consistent with the LVE properties and with the existing literature,[17] these materials have a fixed number of entanglements per chain and a similar number of Kuhn segments per entanglement. It was shown that the sample with a short side group like poly(methyl methacrylate) (PMMA) has a more prominent strain-rate-thinning exponent compared to those with a long side group like poly(hexyl methacrylate) (PHMA).

Thus, these different experimental studies have revealed that the nonlinear extensional rheology of concentrated polymeric liquids is highly sensitive to the chemical structures of monomers and their compositions. As a result, one would expect no universal behavior to exist for these different samples. However, the transition from universality in the equilibrium state to nonuniversality in the nonequilibrium state still needs further clarification.

The mechanism of nonuniversality in the nonlinear extensional rheology has been discussed intensively in the literature.[18−22] Among those studies, the prevalent idea is to refer to the variation of frictional coefficient, representing the effective interchain interaction at the segmental level. In particular, the concept of stretch/orientation-induced reduction of friction (SORF) was proposed by Ianniruberto et al.[20,21] and Yaoita et al.[22] The essential idea of SORF is that in a highly strained polymer melt, an elongated chain can diffuse more smoothly along the orientated direction of the matrix due to the coalignment of segments, indicating a decrease of the apparent frictional coefficient. Based on this concept, it was then proposed[21,23] that polymeric liquids that can exhibit a similar nonlinear extensional rheology should have (i) the same number of entanglements per chain, (ii) the same extensibility of the entanglement strand, and (iii) the same magnitude of friction reduction. While the first two factors can be controlled by molar mass and concentration of the sample, what are the material parameters to determine the friction reduction? In the works by Ianniruberto et al.[21] and Yaoita et al.,[22] the reduction of the frictional coefficient is thought to be a local phenomenon, and thus, it should depend on the order parameters of the segment[21] or a stretch/orientation parameter.[22] The corresponding functional forms can be derived from either the rheo-birefringence data[21] or the decay of stress after the cessation of the flow.[22] These SORF functions are then accounted for in some mechanical models for polymer rheology like the tube-based model,[17] the single-chain bead−rod model,[24] and the multichain slip-link model,[25] and quantitative agreements with the experimental data were successfully obtained.

While the SORF concept provides a helpful way to understand the experimental data, it does not seem to allow for a universal description of the extensional rheology for polymers with different chemistries. For example, in a follow-up work by Masubuchi et al.,[25] the SORF function derived from PS does not work equally well with other samples. Nevertheless, in a more recent work,[26] Masubuchi and his co-workers successfully modeled the extensional rheology of the poly(propylene carbonate) (PPC) melt with the SORF function adjusted for

https://doi.org/10.1021/acs.macromol.3c02648
Macromolecules 2024, 57, 5520−5532

PS. Thus, their function could contain some universal aspects of the polymer melt. However, the central question remains: can we predict friction reduction from the sample's chemical structure?

To understand the role of the chemical structure in nonlinear rheology, we can go back to Figure 1 and focus on the nonequilibrium state in (b). When the melt is subject to a very fast flow, the difference between the spherical and triangle segments will probably emerge when the characteristic time scale of the flow becomes comparable to that of the segment. The interchain interaction will be affected by the shape of the segment, so nonuniversal macroscopic behavior is expected. However, other factors also matter. When the polymer chains are deformed, the configuration of the polymers changes from a random coil to an anisotropic state, and the whole system becomes highly orientated. At the same time, the chain's stacking is readjusted and the magnitude of chain interpenetration is significantly decreased in the melt of deformed polymers. These changes in the large scales also modify the interchain interaction and are intrinsic to the chain-like structure of polymers. They are referred to as the alignment-induced effect, in contrast to the effect of monomer's shape. Moreover, it can be speculated that it should be possible to account for this alignment-induced effect at the level of a Kuhn segment. As a result, the effect of monomer's chemistry on nonlinear extensional rheology should be discussed at two levels: the Kuhn-scale properties that determine the alignment-induced effect and the segmental interactions. While these two factors are always coupled, the alignment-induced effect is expected to be the dominant factor if the flow is not too fast. This would mean that in this flow regime, a universal behavior could potentially exist.

To better explain the transition of polymer dynamics from the universal to the nonuniversal regime, it would be helpful to decouple the effect of chain alignment and the effect of segmental interaction because, currently, it is still unclear from which point the segmental interactions start to make a difference. In this line, using coarse-grained (CG) molecular dynamics (MD) simulation will be helpful.

CG MD simulations have been widely used to investigate the dynamics of polymers.[27−31] In particular, the Kremer−Grest (KG) simulation model[29] with only hard-sphere beads and finite extensible bonds has become the "standard model" to investigate the dynamics of polymer melts. In a recent work by Everaers et al.,[30] it was further justified that this simple model with only an additional bending potential parameter can match the entanglement features of a wide range of commodity polymer melts like the plateau modulus. Indeed, for some properties of the polymers, like the crystalline structure, the detailed force field between the simulation particles is a crucial ingredient of simulation.[27] However, here, the reasoning for using the CG polymer model in replacement of the full atomistic model is rooted in the theoretical fundamental of polymer dynamics as mentioned at the beginning of this work: the detailed chemical structure is always a trivial factor compared to the large-scale dynamics of the polymer chain, at least for the LVE property. When we perform nonequilibrium (NE) MD simulation with CG chain models, it can be speculated that the agreement between the simulation and the experimental data in their extensional rheology will not be very satisfying because experimental facts have suggested that the detailed chemical structure cannot be neglected. However, at the same time, in the CG simulations, the Kuhn segments are structureless objects and interact with each other via a smoothed-out potential. In other words, we can adjust the Kuhn-scale properties of the CG simulation, like the Kuhn length and the packing length, without introducing any extra chemistry-specified interactions at the segmental level. This means that the alignment-induced effect dominates the interchain interaction in the CG MD simulations in a wider window of flow rates, and thus, it should be easier to identify the potential connections between the nonlinear rheology and the Kuhn-scale properties. In the literature, CG simulations have been used to investigate some universal aspects of nonlinear extensional rheology in entangled polymer melts.[32,33] In this study, we will show that CG simulation can also be used as a predictive tool in the current discussions of extensional rheology.

The objective of this work is 2-fold. The first objective is to prove the existence of universal extensional rheology in CG MD simulations. The second is to show how these findings based on simulation data could be beneficial for future studies on experimental samples. A so-called "universal behavior" must be validated by experiments. To this end, the variation of interchain interaction in the simulations will also be investigated in terms of the frictional coefficient to track the determinant factors of extensional rheology. However, a picture different from the SORF concept[20−22] will be proposed. This work should therefore help us to address the remaining question: which kind of polymeric liquids can behave similarly in both the LVE and nonlinear extensional rheology? In a previous study, Wingstrand et al.[23] reported a recipe to mimic the rheology of PS melt from the solution of PMMA diluted by its oligomers. However, the same level of agreement has not been systematically reproduced in other samples. The purpose of the current study is to see if and how the variation of the frictional coefficient can be controlled from only the Kuhn-scale properties, as this would provide clear guidelines in predicting the nonlinear extensional rheology of experimental samples.

It must be noted that this work will only focus on the unentangled or poorly entangled simulation systems because the nonuniversal feature explained by frictional coefficient should not depend on the entanglement state of the material. To quantify the variation of the frictional coefficient in the simulation, we will refer to the approach proposed very recently by our group.[34] The general idea is the following. In an unentangled melt, it is assumed that the dynamics of a test chain can always be mimicked by the Langevin equation of the BSC model, as long as the parameters defined in this model, including the spring coefficient, the monomeric frictional coefficient, and the Brownian intensity, are properly adjusted. Thanks to the analytical structure of the dynamic equation, those adjustable parameters, also called the NE parameters, can be expressed as some explicit functions of the rheological and structural properties. For example, the relative variation of the frictional coefficient under extensional flow can always be expressed as a function of the normalized extensional viscosity and the mean-squared radius of gyration.[34] In this way, the frictional coefficient can be inversely deduced from the macroscopic properties of an unentangled system. This approach was first proposed by Watanabe and his co-workers.[35−38] We extended this idea by making use of the rheological and structural properties that can be observed in the simulations.[34] These frictional coefficients obtained for different simulation systems are then compared to propose a Kuhn-scale criterion of extensional viscosity that can be tested experimentally.

https://doi.org/10.1021/acs.macromol.3c02648
Macromolecules 2024, 57, 5520−5532

Table 1. Description of the Simulation Systems and Their Kuhn-scale Properties[a]

label	N_m	κ	ρ_m	$\langle R_0^2 \rangle$	τ_R	N_k	l_k	p	n_k
L10-nk2	10	0.00	0.85	12.98	29	5.81	1.49	0.82	1.83
L20-nk2	20	0.00	0.85	29.17	131	11.53	1.59	0.77	2.08
L50-nk2	50	0.00	0.85	78.90	1330	29.47	1.64	0.74	2.20
L60-nk3	60	0.50	0.85	110.47	2611	30.35	1.91	0.64	2.99
L70-nk4	70	1.00	0.85	154.84	5425	29.47	2.29	0.53	4.31
L86-nk6	86	1.50	0.85	228.44	18,717	30.15	2.75	0.44	6.21
L100-nk2	100	1.30	0.21	313.55	274	29.70	3.25	1.52	2.14
L100-nk3	100	1.50	0.30	311.81	517	29.87	3.23	1.07	3.02
L100-nk4	100	1.75	0.42	315.69	1824	29.50	3.27	0.75	4.34
L100-nk6	100	1.85	0.63	308.63	8360	30.17	3.20	0.51	6.22
S3Arm25	76	0.0	0.85		1170				2.20[b]
S4Arm25	101	0.0	0.85		1465				

[a] N_m, number of beads per chain; κ, bending parameter; $\langle R_0^2 \rangle$, equilibrium mean-squared end-to-end distance; τ_R, Rouse time; N_k, number of Kuhn segments per chain; l_k, Kuhn length; p, packing length defined as $p \equiv (N_m/\rho_m)/\langle R_0^2 \rangle$; n_k, reduced Kuhn density as defined in eq 4. [b] The Kuhn scale description of the star-like polymers is expected to be similar to their linear counterpart.

The rest of this work is organized as follows. In Section 2, the methods of CG MD simulation are explained, and some equilibrium static and dynamic properties of the simulations are given. In Section 3, the nonlinear extensional rheology of the simulations is discussed and compared with the experimental data. Then, the derivation of the expressions to quantify the frictional coefficient is explained and the validity of these expressions is proved. After that, it is shown the frictional coefficients are found to be universally related to the projection area of the polymer coil. It is then explained how this relationship leads to a criterion of extensional viscosity and how the simulation and specific experimental data support it. The conclusions are summarized in Section 4.

2. SIMULATION METHODS

The simulation data to be analyzed in this work are also based on the KG simulation model.[29] The simulation details can be found in the literature and our previous work.[34] They are briefly summarized here. The KG simulation model is composed of coarse-grained beads interacting with each other via the pure repulsive 6−12 LJ potential with a cutoff distance of $r_c = 2^{1/6}$, at a reduced number density $\rho_m = 0.85$. (the standard LJ unit system is used, and all quantities are expressed relative to the length and energetic parameters in the LJ potential). The present study will also discuss the simulation systems with other densities. The segments are connected by the FENE potential: $U_{FENE}(r) = -kR_0^2/2\ln[1 - (r/R_0)^2]$ for $r < R_0$, where $k = 30$ and $R_0 = 1.50$. In this work, we will also modify the number of beads per Kuhn segment via the bending potential: $U_{bend}(\Theta) = \kappa(1 - \cos\Theta)$, where Θ is the angle between two subsequent bonds.

The NEMD simulation is carried out from the SLLOD equation of motion with a Nosé−Hoover thermostat for the canonical (NVT) ensemble,[39] as implemented in the LAMMPS simulation software.[40] The governing equations of motion are[39]

$$\begin{aligned} \dot{\boldsymbol{r}}_i &= \frac{\boldsymbol{p}_i}{m_i} + \boldsymbol{r}_i \cdot \mathbf{K} \\ \dot{\boldsymbol{p}}_i &= \boldsymbol{F}_i - \boldsymbol{p}_i \cdot \mathbf{K} - \nu^{(\mathrm{NH})} \xi \boldsymbol{p}_i \\ \dot{\xi} &= \nu^{(\mathrm{NH})} \left(\frac{T}{T_0} - 1 \right) \end{aligned} \tag{1}$$

where $\boldsymbol{r}_i$ is the positional vector of a bead and $\boldsymbol{p}_i$ is the peculiar momentum relative to the stream velocity ($\boldsymbol{r}_i \cdot \mathbf{K}$ in eqn 1). $\boldsymbol{F}_i$ is the total force. The flow gradient tensors $\mathbf{K}$ to be investigated in this work are

$$\begin{aligned} \mathbf{K}_{shear} &= \begin{bmatrix} 0 & \dot{\gamma} & 0 \\ 0 & 0 & 0 \\ 0 & 0 & 0 \end{bmatrix}; \\ \mathbf{K}_{pext} &= \begin{bmatrix} \dot{\varepsilon} & 0 & 0 \\ 0 & -\dot{\varepsilon} & 0 \\ 0 & 0 & 0 \end{bmatrix}; \\ \mathbf{K}_{uniext} &= \begin{bmatrix} \dot{\varepsilon} & 0 & 0 \\ 0 & -\dot{\varepsilon}/2 & 0 \\ 0 & 0 & -\dot{\varepsilon}/2 \end{bmatrix} \end{aligned} \tag{2}$$

where "pext" and "uniext" are the abbreviations for planar and uniaxial extensions, respectively. To be consistent with the flow geometry in the SLLOD equation of motion, the Lees−Edwards periodic boundary condition (PBC) is used for shear flows.[41] The generalized Kraynik−Reinelt PBC is used for extensional flows (uniaxial and planar extensions).[42,43] In the Nosé−Hoover thermostat, T is the instant kinetic temperature defined from the motion relative to the stream velocity. T_0 is the target temperature. The rate of coupling with the heat bath is controlled by the parameter $\nu^{(\mathrm{NH})}$, which is set to be $1/\nu^{(\mathrm{NH})} = 100\Delta t$. $\Delta t = 0.001$−0.01 is the time step of simulation. Each simulation box is composed of 500 chains. In our previous work,[34] we have presented direct comparisons between our NEMD simulation data and the results in the existing literature of the same systems, and the quantitative agreement between them has been confirmed.

The descriptions of the simulation systems are listed in Table 1. Most simulations are designed to have a similar number of Kuhn segments per chain $N_k \approx 30$ for comparison with the experimental data in a later section. However, the bending parameters and the monomer densities are different in these systems, mimicking the difference in chemistry. To choose the bending parameter for a desired property, we can refer to the calculators given by Svaneborg and Everaers,[31] but the values listed in Table 1 are mostly from our calculations. Based on the primitive path analysis on the standard KG simulation model in the previous studies,[31,44] all the systems except L86-nk6 and L100-nk6 are in the unentangled regime ($N_k < 2N_{ek}$, where N_{ek} is the number of Kuhn segments per entanglement strand). L86-nk6 and L100-nk6 are weakly entangled with $N_k/N_{ek} \approx 3$. The entangled samples and the star-like polymers with 3 and 4 arms per chain and fixed arm length (S3Arm25 and S4Arm25) are included to broaden the discussion.

For the LVE properties of the systems, the linear relaxation modulus $G(t)$ is calculated from the time correlation functions of the stress components using the multitau correlator algorithm.[45] The simulation results of the L50-nk2 sample have been presented in our previous work.[34] The linear envelope of the shear viscosity growth function $\eta^+_{LVE}(t)$ is obtained by integrating $G(t)$ with time and the zero-shear viscosity η_0 is the plateau value of $\eta^+_{LVE}(t)$. To show the universal feature

https://doi.org/10.1021/acs.macromol.3c02648
Macromolecules 2024, 57, 5520−5532

of the systems in their LVE properties, the relaxation moduli in the time domain are transformed into the complex moduli in the frequency domain. To do this, the i-Rheo *GT* toolkit proposed by Tassieri et al.[46] is used. In this toolkit, the linear relaxation modulus from simulation, which is discrete and nonlinearly distributed in the time domain, is oversampled first before being transformed to the frequency domain. More details of this toolkit can be found in the original paper,[46] where the validity of the methods in dealing with the $G(t)$ data of the KG simulation model has also been demonstrated. For the clarity of the terminal regime in the complex modulus, the relaxation modulus from our simulations is truncated at a specific time t_c and $G(t > t_c)$ is set to zero, where $\eta^+_{LVE}(t_c)$ is in its plateau regime.

In Figure 2, the storage and loss moduli, $G'(\omega)$ and $G''(\omega)$, of the unentangled simulations with a similar number of Kuhn segments per chain ($N_k \approx 30$) are presented. To superpose the data, the moduli are rescaled by the number density of polymer chains $c \equiv \rho_m/N_m$ and the reduced temperature k_BT. For comparison with the experiment in a later section, the Rouse time τ_R of the simulation is evaluated from the following expression that has been used for the experimental data[15]

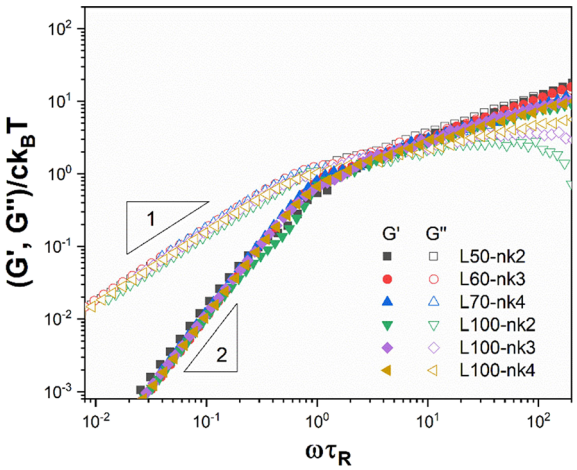

Figure 2. Storage and loss moduli of the unentangled simulations with similar Kuhn segments per chain ($N_k \approx 30$). The complex moduli are transferred from the linear relaxation moduli using the i-Rheo *GT* toolkit.[46] The moduli are normalized by the number density of polymer chains c and the reduced temperature k_BT.

$$\tau_R \approx \frac{15}{\pi^2}\langle\tau\rangle = \frac{15}{\pi^2}\left[\frac{G'}{\omega G''}\right]_{\omega\to 0} \quad (3)$$

The Rouse time calculated from eq 3 is smaller than that from the Rouse mode analysis (RMA)[47,48] by a factor of 2 to 3 ($\tau_R \approx 3240$ from RMA was used for the sample L50-nk2 in our previous work[34]). It can be seen from Figure 2 that all the moduli are well-superposed, and no plateau is observed in the storage modulus. Thus, the unentangled states of these samples and the universal feature of the LVE are well confirmed. For the entangled samples, the Rouse time for L86-nk6 is estimated from a calculator by Svaneborg and Everaers:[31] $\tau_R \approx N_k^2 l_k^3$, while τ_R for L100-nk6 is estimated by horizontally shifting its normalized extensional viscosity so that its maximum appears in the same Rouse Weissenberg number as the L86-nk6 sample.

Recently, Everaers et al.[30] suggested that the KG simulation model can be related to the commodity polymers based on their Kuhn-scale properties and the prediction of the Lin−Noolandi theory of entanglement.[2−4] The essential quantity to make the connections is the reduced Kuhn density n_k, also termed the "Kuhn number" in that work.[30] This dimensionless quantity is defined as the number of Kuhn segments within the volume of a Kuhn length cube or the ratio of the Kuhn length l_K and the packing length p. That is

$$n_k \equiv cN_K l_K^3 = \frac{l_K}{p} = \frac{\rho_m\langle R_0^2\rangle^2}{N_m L} \quad (4)$$

The product cN_K represents the number density of Kuhn segments. In the rightmost expression of eq 4, L is the contour length of the chain. The reduced Kuhn density is a material parameter and thus also represents the chemical aspect of the sample. According to the Lin−Noolandi theory,[2−4] both the reduced entanglement modulus $G_N^0 l_K^3/k_BT$ and the number of Kuhn segments per entanglement N_{ek} can be expressed as universal functions of n_k. In the standard KG simulation model, n_k can be adjusted from only the bending parameter κ. Thus, it was proposed by Everaers et al.[30] that focusing on n_k provides the opportunity to simulate all the commodity materials from the KG model. A specific value of the bending parameter κ was also suggested for each chemistry. This idea is appealing to fulfill the objectives of this work about extensional rheology. In addition, the potential impact of n_k on the nonlinear rheology was also mentioned by Everaers et al.[30] However, no details were provided and the Lin−Noolandi theory of entanglement does not predict the segmental friction and the nonlinear extensional rheology of unentangled samples. Considering the convenience and the potential impact of the reduced Kuhn density, this quantity will be discussed and the values of n_k for the different simulation systems investigated in this work are also included in Table 1. In the following sections, it will be shown that the importance of this Kuhn-scale property for rationalizing the nonlinear extensional properties is indeed supported by our simulation data.

3. RESULTS AND DISCUSSION

3.1. Nonlinear Extensional Rheology of the Simulations and the Comparison with Experimental Data. Before presenting the analysis of the frictional coefficients, there are some crucial points to justify. The first point to discuss is how the chemistry affects the extensional rheology in the CG MD simulations and how the simulation results compare with the experimental data of the unentangled PS and PtBS melts from Matsumiya et al.[15] when they have a similar number of Kuhn segments per chain ($N_k \approx 30$). In this part, we will focus on the simulations with the standard monomer density $\rho_m = 0.85$, but different bending potentials (L50-nk2, L60-nk3, L70-nk4, and L86-nk6).

In Figure 3, the normalized steady-state extensional viscosities η_E/η_{E0} under uniaxial extensional flow are plotted as a function of the reduced extensional rate $\dot{\epsilon}\tau_R$. In this plot, the viscosities of all the simulations show thickening followed by thinning, like the experimental observation by Matsumiya et al.[15] At the same time, we can identify the effect of chain rigidity. The melt with the most flexible chains (L50-nk2 with $\kappa = 0$) has the most thickened viscosity compared to the value of the LVE limit. With increasing chain rigidity, the maximum value of η_E/η_{E0} is decreased. The idea of SORF may explain this rigidity effect:[21,22] The more rigid chains are more inclined to be orientated locally and thus exhibit more friction reduction. However, we could also relate this observation with other properties. From the Kuhn-scale properties of these simulation systems, as listed in Table 1, we may see that all these properties, including Kuhn length l_k, packing length p, as well as reduced Kuhn density n_k, can be the candidates to explain the profile of η_E/η_{E0}. However, we cannot conclude yet which factor is the determinant at the present stage.

When comparing the simulations with the experimental data by Matsumiya et al.,[15] the simulation results are in the comparable range with the experiment data. In particular, the viscosity profile of the L70-nk4 simulation sample almost quantitatively reproduces the unentangled PtBS up to the flow rate $\dot{\epsilon}\tau_R \approx 10$. In contrast, the discrepancy between the

https://doi.org/10.1021/acs.macromol.3c02648
Macromolecules 2024, 57, 5520−5532

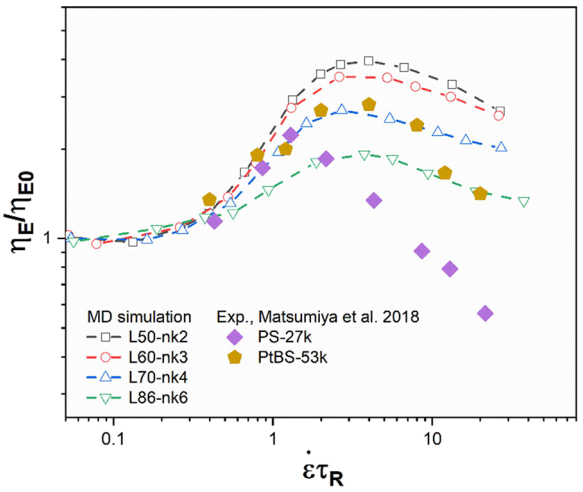

Figure 3. Normalized steady-state extensional viscosity under uniaxial extensional flows of the CG MD simulations and the experimental data of the unentangled PS and PtBS melts from Matsumiya et al.[15] The simulations have the same monomer density $\rho_m = 0.85$ and a fixed number of Kuhn segments per chain $N_k \approx 30$, but the chain rigidity is different, as listed in Table 1. The values of N_k are 30 for PS and 35 for PtBS.[15]

simulations and the unentangled PS sample is much more significant. Interestingly, the value of reduced Kuhn density n_k of PtBS is around 4.73 from the handbook by Fetters et al.,[17] which is very close to the L70-nk4 simulation sample ($n_k \approx 4.31$). This means that n_k is potentially the critical parameter to relate simulation and experimental sample in their nonlinear extensional rheology. However, we should not conclude from a single group of data. From the simulation side, although the standard KG simulation model is widely used, it does not mean the results should represent the CG simulation models using different force fields. On the other side, PS has a reduced Kuhn density close to PtBS ($n_k \approx 4.54$ for atactic PS[17,30]). Thus, the reduced Kuhn density n_k cannot explain the difference between PS and PtBS. Nevertheless, the comparison between simulation and experiment provides a clue in analyzing the nonlinear extensional rheology data. Moreover, based on the future analysis of the simulations in the following sections, the agreement between simulation and PtBS is probably not a coincidence.

3.2. Expressions to Quantify the Mean-Field Frictional Coefficient. In this section, the expressions to quantify the mean-field frictional coefficient are presented. Before using them to analyze the frictional coefficient of the simulations, it is also important to validate their effectiveness. In the previous study,[34] we considered all the NE parameters defined in the BSC model and solved the steady-state solutions of the dynamic equation from the corresponding eigenmodes. However, this method unavoidably involves some approximations of the NE parameters. This section presents a more straightforward way of deriving the frictional coefficients. As explained in Section 1, the standing point is that the interchain interaction in the unentangled melts can be simplified into a frictional coefficient. Thus, the dynamics of a test chain can always be described by the following Langevin equation of the BSC model:

$$\boldsymbol{\zeta}\cdot\left[\frac{\mathrm{d}\boldsymbol{r}_n}{\mathrm{d}t} - \mathbf{K}\cdot\boldsymbol{r}_n\right] = -\sum_{m=0}^{N} a_{mn}\left(\boldsymbol{r}_m - \boldsymbol{r}_n\right) + \boldsymbol{F}_B \tag{5}$$

This work uses a slightly different notation system from our previous work.[34] $\boldsymbol{r}_n$ represents the positional vector of the nth bead in the model, where the bead index ranges from 0 to N. a_{mn} is the spring coefficient of the connector $\boldsymbol{r}_m - \boldsymbol{r}_n$ when the two beads are connected. Otherwise, it will be zero. This means that eq 5 describes an arbitrary chain architecture, not just the linear chain. The Brownian force $\boldsymbol{F}_B$ has a zero first-moment average but a nonzero second-moment average, which does not necessarily follow the fluctuation−dissipation theorem (FDT) in the melt under flows. The frictional coefficient $\boldsymbol{\zeta}$ in eq 5 is in the tensorial form to account for the anisotropic effect. Its dependence on the bead index is ignored. It is also considered as a decoupled quantity with a negligible memory effect. Thus, eq 5 may not be the most precise expression for describing the dynamic behavior of a test chain in a melt. However, these simplifications would be acceptable since we will discuss the condition in the mean-field limit. For the rheological and structural properties, the mean-squared radius of gyration tensor $\langle \mathbf{R}_g^2 \rangle$ and the stress tensor $\boldsymbol{\sigma}$ are defined as

$$\langle \mathbf{R}_g^2 \rangle \equiv \frac{1}{N+1}\sum_{n=0}^{N} \langle (\boldsymbol{r}_n - \boldsymbol{r}_{cm})(\boldsymbol{r}_n - \boldsymbol{r}_{cm}) \rangle \tag{6}$$

$$\begin{aligned}\boldsymbol{\sigma} &\equiv c\sum_{m=0}^{N}\sum_{n=0}^{m} \langle a_{mn}(\boldsymbol{r}_m - \boldsymbol{r}_n)(\boldsymbol{r}_m - \boldsymbol{r}_n) \rangle \\ &= -c\sum_{m=0}^{N}\sum_{n=0}^{n} \langle a_{mn}(\boldsymbol{r}_m - \boldsymbol{r}_n)\boldsymbol{r}_n \rangle\end{aligned} \tag{7}$$

where $\boldsymbol{r}_{cm}$ is the center of mass of the chain. Based on the definition of a_{mn}, eq 7 is the expression of stress for general chain architectures.

Combining eqs 5−7, we can write the time evolution equation of $\langle \mathbf{R}_g^2 \rangle$ as

$$\begin{aligned}\langle \mathbf{R}_g^2 \rangle_{(1)} = &\frac{1}{c(N+1)}(\boldsymbol{\zeta}^{-1}\cdot\boldsymbol{\sigma} + \boldsymbol{\sigma}\cdot\boldsymbol{\zeta}^{-1}) + \frac{1}{N+1} \\ &(\boldsymbol{\zeta}^{-1}\cdot\langle \boldsymbol{F}_B\boldsymbol{F}_B \rangle\cdot\boldsymbol{\zeta}^{-1})\end{aligned} \tag{8}$$

where $(\cdots)_{(1)} = \mathrm{d}(\cdots)/\mathrm{d}t - \mathbf{K}\cdot(\cdots) - (\cdots)\cdot\mathbf{K}^{\dagger}$ is the upper-convected time derivative as defined in the textbook.[49] Equation 8 is also known as the expression of stress of the Giesekus form,[49] in the case that the frictional coefficient is a scalar quantity and the Brownian force satisfies the FDT. When the frictional coefficient $\boldsymbol{\zeta}$ is defined as a decoupled quantity, the derivation from eqs 5−8 is rigorous, and no assumptions have been made for the spring coefficient a_{mn}. This means that even if the spring coefficient is coupled with the instant elongation of the spring and has a stochastic nature in the model, the dynamics will still precisely follow eq 8. In particular, in the case of a chain model with a rigid constraint like Kramers's bead−rod chain model, we can also derive eq 8 starting from the Fokker−Plank equation of its orientational distribution function.[49] The derivation in the simplest rigid dumbbell model is shown in Section A of the Supporting Information. The second term on the right side of eq 8, which represents the contribution of the Brownian force, is relatively small compared to that from the intramolecular elastic force, which is the first term on the right side of eq 8. This is especially true when we consider the case of extensional flow or when we focus on the anisotropic part of this equation. In this case, whether or not the model assumes the validity of FDT will not make a significant difference.

https://doi.org/10.1021/acs.macromol.3c02648
Macromolecules 2024, 57, 5520−5532

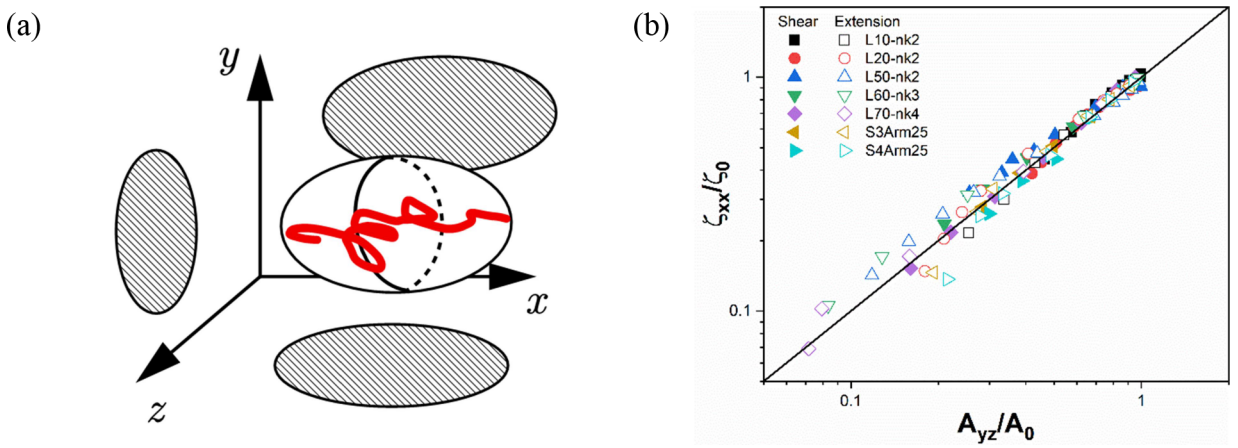

Figure 4. (a) Illustration of the projection area of the polymer coil. (b) Variation of the frictional coefficient in the aligned direction ζ_{xx} as a function of the projection area in the plane normal to the x-axis A_{yz}, normalized by the corresponding values under equilibrium. Different symbol interiors mean different types of flow.

The expressions that relate the variation of the frictional coefficient with the rheological and structural properties can be obtained after substituting the flow gradient tensors in eq 2 into eq 8. They are

$$\text{Shear: } \frac{\zeta_{xx}}{\zeta_0} \approx \frac{\Psi_1/\Psi_{10}}{\Gamma/\Gamma_0} \tag{9}$$

$$\text{Planar extension: } \frac{\zeta_{xx}}{\zeta_0} \approx \frac{2\eta_E/\eta_{E0} - \eta_C/\eta_{C0}}{\langle R^2_{gxx}\rangle/\langle R^2_{gxx}\rangle_0} \tag{10}$$

$$\text{Uniaxial extension: } \frac{\zeta_{xx}}{\zeta_0} \approx \frac{3}{2}\frac{\eta_E/\eta_{E0} - 1/3}{\langle R^2_{gxx}\rangle/\langle R^2_{gxx}\rangle_0} \tag{11}$$

All the subscripts "0" mean the corresponding values under equilibrium. The components of the stress tensor, the radius of gyration tensor, and the frictional tensor are unbolded with their respective subscripts. The flow geometries defined in eq 2 indicate that polymers are elongated in the x direction in all kinds of flows. In eq 9, $\Psi_1 = -(\sigma_{xx} - \sigma_{yy})/\dot{\gamma}^2$ is the first normal coefficient. $\Gamma = \langle R^2_{gxy}\rangle/\dot{\gamma}$ is a structural quantity whose definition is similar to the shear viscosity. In eq 10, $\eta_C = -(\sigma_{yy} - \sigma_{zz})/\dot{\varepsilon}$ is the cross viscosity. In the simulations, all the values from eqs 9−11 decrease with deformation. For the two types of extensional flow, eq 10 for planar extension is nearly rigorous. In eq 11 for uniaxial extension, the variations of NE parameters in the contraction directions are ignored. The variations of the frictional coefficient from eqs 10 and 11 are found to be close under the same extensional rate.[34] From eq 8, it is also possible to derive the expressions for other components of the frictional coefficient tensor. However, the corresponding values are less reliable because the calculation involves some strongly fluctuating quantities. Thus, this work only focuses on the friction in the elongation direction that decreases significantly with flows.

To further validate the above expressions, we conducted single-chain stochastic simulations of the BSC model described in Section B of Supporting Information. In the stochastic simulations, the "input" values of the frictional coefficients defined in the model are directly compared with the "output" values from eqs 9 and 10. The comparison reveals a quantitative agreement between the two groups of values as long as the frictional coefficient is defined as a mean-field quantity.

In the original approach by Watanabe and his co-workers,[35−38] the authors combined rheology and dielectric relaxation to quantify the frictional coefficient of an experimental sample. Our expressions from eqs 9−11 involve some delicate structural properties that may be easily obtained from the simulations but will require large-scale facilities to perform neutron scattering experiments[50,51] for experimental samples. However, as it will be pointed out later, it is still possible to make predictions on the nonlinear extensional rheology even if the frictional coefficients are not explicitly characterized in the materials.

3.3. Universal Relation between the Frictional Coefficient and the Projection Area of the Polymer Coil in Unentangled Melts. In this section, the dependence of the frictional coefficients on the molecular structures in the simulations will be discussed. In our previous work,[34] we have presented the variation of the frictional coefficient of the simulations with flexible chains ($\kappa = 0$) as a function of the strain rate. It was found that there is an apparent scaling for the friction: $\zeta_{xx} \sim (\tau_R\dot{\varepsilon})^{-1/2}$ for extension and $\zeta_{xx} \sim (\tau_R\dot{\gamma})^{-1/4}$ for shear. The next point to address is what kind of property can explain those frictional coefficients.

It must be noted here that in our previous work,[34] we have tested the SORF function proposed by Ianniruberto et al.[24,52] and found it effective for the simulation data with flexible chains. Therefore, the relation proposed below is not the only way, but one of the possibilities to describe the results in a unified form. Here, we introduce an intuitive idea to consider the determinant for the frictional coefficient. As shown in Figure 4a, when polymers are elongated along the x-axis, their dimensions in the other two directions shrink simultaneously, resulting in a smaller projection area in the yz-plane. This leads to fewer collisions with other chains when the polymer coil diffuses along the x-axis. Hence, it is reasonable to consider the variation of the frictional coefficient in terms of the projection area. This relationship has been proposed in an early study on the liquid crystal dynamics.[53] Indeed, polymer melts under flow conditions have an ordering similar to the nematic liquid crystals, so it is logical to think about their connections. However, to the current author's knowledge, this relationship has not been applied to polymer dynamics.

The projection areas of a polymer coil can be directly estimated from its mean-squared radius of gyration tensor as

https://doi.org/10.1021/acs.macromol.3c02648
Macromolecules 2024, 57, 5520−5532

$$\mathbf{A}_{\text{proj}} \approx [\det(\langle \mathbf{R}_g^2 \rangle)\langle \mathbf{R}_g^2 \rangle^{-1}]^{1/2} = [\text{adj}(\langle \mathbf{R}_g^2 \rangle)]^{1/2} \quad (12)$$

where $\det(\langle \mathbf{R}_g^2 \rangle)$ means the determinant of $\langle \mathbf{R}_g^2 \rangle$. Its square root is usually considered as the pervading volume of the coil. The product of the determinant and the inverse of a matrix is the definition of the so-called adjugate matrix in linear algebra. The square root of a matrix can be decomposed as

$$\mathbf{B}^{1/2} = \mathbf{T}^{-1} \cdot \mathbf{\Lambda}^{1/2} \cdot \mathbf{T} \quad (13)$$

where $\mathbf{\Lambda}$ is the eigenvalue matrix of $\mathbf{B}$ and $\mathbf{T}$ is the matrix containing all the eigenvectors. Because $\langle \mathbf{R}_g^2 \rangle$ is always positively definite, this square root calculation is possible in general cases. When the off-diagonal terms in $\langle \mathbf{R}_g^2 \rangle$ are all equal to zero, it can be easily proved that eq 12 shows the projection area in the plane normal to the corresponding axis. When $\langle \mathbf{R}_g^2 \rangle$ has nonzero off-diagonal terms like the case of shear flow, eq 12 also gives a reasonable estimation. The eigenvalues of $\langle \mathbf{R}_g^2 \rangle$ represent the three principal axes of an ellipse object. At the same time, the eigenvectors are the rotational operation to make the longest axis parallel to the x-axis of the laboratory frame.

The frictional coefficients calculated from eqs 9 and 10 are then plotted as a function of corresponding projection areas based on eq 12, as shown in Figure 4b. This figure includes the simulation data of the unentangled systems which differ in (i) the number of Kuhn segments per chain; (ii) the Kuhn-scale properties (Kuhn length and packing length determined by the bending potential); (iii) the large-scale chain architecture (linear chains and star-like chains); and (iv) the type of flow. Surprisingly, all these data are well-superposed in this plot.

The projection−friction relationship should also be valid in the solutions. If the solute polymers are still interpenetrating with each other when deformed, and if the dynamics of the solvent molecules are well separated from the polymers, the effective interaction acting on a test chain should continue to be governed by the state of alignment with the surrounding chains, while the solvent molecules will provide background friction that does not change with the flows. Some experimental data have shown such a tendency. For example, Shahid et al.[54] found that the absolute steady-state extensional viscosities of semidilute solutions with the same long-chain component and concentration are nearly independent of the solvent molecules under the same extensional rate. Of course, with the increase of flow rate or the decrease of concentration, there will be a point where the dominant factor changes from the chain−chain interaction to the chain−solvent interaction. This can lead to the breakdown of the projection−friction relationship. The solution systems with explicit solvent molecules will be investigated in a future study.

On the other hand, in the case of entangled polymer melts, it is expected that the current projection−friction relationship will not be valid if we consider the configuration of the whole polymer. Indeed, the mean-field frictional coefficient cannot describe the dynamics beyond the length scale of the entanglement strand. When the flow rate is between $1/\tau_d$ and $1/\tau_R$ where τ_d is the disentanglement time, the deformation of the polymer is governed by the reorientation of the primitive path, and the entanglement strand remains undeformed.[1] Thus, the frictional coefficient inside the entanglement strand will not change with the projection area of the whole chain. However, generally, the nonlinear property of the entangled polymer in this flow regime depends on the number of entanglements, which is controlled by the molar mass of the sample rather than the chemistry of the monomer. When the flow is faster than $1/\tau_R$, the nonlinear response of the entanglement strand becomes the determinant factor. In this case, we can expect a potential universal relation between the frictional coefficient and the projection area of the entanglement strand. In fact, the most important point for this projection−friction relationship is that we can derive a Kuhn-scale criterion for describing the extensional viscosity. In particular, the current theory of entanglement, the Lin−Noolandi theory,[2,3] suggests we can extend this criterion derived from the unentangled regime to the entangled regime. This will be discussed in the following section.

3.4. Kuhn-Scale Criterion of Extensional Viscosity Indicated by the Projection−Friction Relationship. The excellent agreement between the frictional coefficient and the projection area shown in Figure 4b not only provides a way to rationalize the observations in the CG simulations, but also confirms a speculation made in Section 1: the alignment-induced variation of interchain interaction can be explained from the large-scale properties, without referring to the details in the small scales. Particularly, based on the projection−friction relationship, a guideline can be derived for designing rheologically analogous samples.

According to eq 11, the normalized extensional viscosity η_E/η_{E0} of an unentangled sample can always be expressed as a function of the reduced frictional coefficient ζ_{xx}/ζ_0 and the reduced chain dimension $\langle R_{gxx}^2 \rangle/\langle R_{gxx}^2 \rangle_0$ in the elongation direction. To explain the dependence of these two quantities, let us consider the scenario of an extremely fast flow. In this case, the polymer takes the shape of a rigid rod, and the frictional coefficient depends on the cross-sectional area, or in other words, the thickness of the polymer thread. Currently, the packing length p is thought to be the measure of effective chain thickness in a concentrated liquid,[55] considering the fluctuations in the radial direction. Therefore, according to the projection−friction relationship, we can write

$$\left.\frac{\zeta_{xx}}{\zeta_0}\right|_{\dot{\varepsilon}\to\infty} \overset{\text{projection - friction}}{\simeq} \frac{p^2}{\langle R_g^2 \rangle_0} \simeq \frac{1}{N_k n_k^2} \quad (14)$$

where the prefactors are ignored. Equation 14 shows that the reduced frictional coefficient in the ultrafast flow limit depends on the packing length, the Kuhn length, and the number of Kuhn segments. However, the two length scales can be simplified as the reduced Kuhn density. In contrast, the variation of chain dimension is the difference between the random coil and the rigid rod, which is determined by the number of Kuhn segments:[56]

$$\left.\frac{\langle R_{gxx}^2 \rangle}{\langle R_{gxx}^2 \rangle_0}\right|_{\dot{\varepsilon}\to\infty} \simeq \frac{N_k^2 l_k^2}{N_k l_k^2} \simeq N_k \quad (15)$$

Inspired by the expressions in the extreme case, it can be speculated that under an arbitrary extensional rate $\dot{\varepsilon}\tau_R$, ζ_{xx}/ζ_0 and $\langle R_{gxx}^2 \rangle/\langle R_{gxx}^2 \rangle_0$ could be expressed as

$$\frac{\zeta_{xx}}{\zeta_0} = \frac{\zeta_{xx}}{\zeta_0}(\dot{\varepsilon}\tau_R, N_k, n_k) \quad (16)$$

$$\frac{\langle R_{gxx}^2 \rangle}{\langle R_{gxx}^2 \rangle_0} = \frac{\langle R_{gxx}^2 \rangle}{\langle R_{gxx}^2 \rangle_0}(\dot{\varepsilon}\tau_R, N_k) \quad (17)$$

Combining eqs 11, 16, and 17, the normalized extensional viscosity will be expressed as

https://doi.org/10.1021/acs.macromol.3c02648
Macromolecules 2024, 57, 5520−5532

$$\frac{\eta_E}{\eta_{E0}} = \frac{\eta_E}{\eta_{E0}}(\dot{\varepsilon}\tau_R, N_k, n_k) \tag{18}$$

This means that if the materials of different chemistries have the same number of Kuhn segments per chain and the same reduced Kuhn density, we should observe the same normalized extensional viscosity at a given Rouse Weissenberg number, representing the universal feature of extensional rheology. Most importantly, eq 18 can be directly tested from experiments because all the ingredients in this expression are accessible. Especially the value of the reduced Kuhn density of specific chemistry can be found in the current polymer handbook[17] and in the work by Everaers et al.[30] For the choice of experimental samples, we can investigate the melts with completely different chemistries but a similar value of n_k. Focusing on the solutions is also reasonable, adjusting carefully the molar mass and concentration. This strategy requires determining n_k as a function of the polymer concentration in different solvents. According to the rightmost definition of n_k in eq 4, we need to consider not only the change of monomer density but also the swelling of the polymer coil in the solution, which has different scaling exponents depending on the quantity of the solvent.[57] In short, eq 18 suggests an explicit and practical way to control the nonlinear extensional rheology of the experimental samples.

Even though the derivation from eqs 14−18 is based on the unentangled melts, we can extend this prediction on extensional viscosity to the entangled samples. According to the Lin−Noolandi theory,[2,3] the number of Kuhn segments per entanglement strand N_{ek} is uniquely determined by the reduced Kuhn density n_k:[30]

$$N_{ek} = \left(\frac{\alpha}{n_k}\right)^2 \tag{19}$$

where $\alpha = 18 \pm 2$ is the universal number of entanglement strands per tube cube in different chemistries. In later theories that are generalized from the Lin−Noolandi ansatz,[55,58,59] N_{ek} is always a universal function of n_k (for flexible chain regime in Milner's theory,[55] where the tube diameter is much larger than the Kuhn length). As a result, when two samples have the same number of Kuhn segments N_k and the same reduced Kuhn density n_k, it has been indicated that they will have the same number of entanglement, which guarantees the universal LVE property as predicted by the tube model.[1] They will also have the same extensibility of the entanglement strand (N_{ek}), which has been proven to be important for nonlinear extensional rheology according to the experiment by Morelly et al.[14] Overall, the Kuhn-scale criterion of extensional viscosity in eq 18 raises an unrecognized relationship between the entanglement property under equilibrium and the nonlinear dynamics of an unentangled sample under fast flows.

While the derivation of eq 18 from eqs 14−17 may appear empirical and rough, it is natural to question the validity of the intermediate steps. Nevertheless, the significance and potential benefits of eq 18 cannot be dismissed. As such, in the upcoming section, its validity is shown from two standpoints. First, eq 18 can be utilized to design liquids with analogous linear and nonlinear rheological properties in simulations. Second, eq 18 can be validated against specific experimental data available in the literature.

3.5. Designing Rheologically Analogous Simulation Systems based on the Kuhn-Scale Criterion. To prove the usefulness of the Kuhn-scale criterion in eq 18, here, a procedure to design rheologically analogous simulation systems is described. The target is to reproduce the extensional viscosity of the simulation samples discussed in Figure 3 (L50-nk2, L60-nk3, L70-nk4, and L86-nk6) from a new set of systems containing polymers of a different chain length ($N_m^* = 100$). The number density of the beads and the bending potential of the chain are adjusted simultaneously to ensure the new systems have the same number of Kuhn segments N_k and the same reduced Kuhn density n_k as the reference systems.

To show the target of our design, $q = N_m^*/N_m^{(ref)}$ is defined as the ratio of the bead number per chain, where the superscript "ref" means the value of the reference sample we plan to mimic. To ensure that the two systems have the same number of Kuhn segments per chain N_k, the ratio of the Kuhn length should satisfy $l_k^*/l_k^{(ref)} = q$, because the ratio of the contour length is also equal to q. Consequently, the new system should have a polymer size of $\langle R_0^2\rangle^* = q^2\langle R_0^2\rangle^{(ref)}$. To maintain a constant value of n_k, the packing length should also be amplified by a factor of q. Therefore, based on the definition of the packing length, the density of segments in the new system should be $\rho_m^* = \rho_m^{(ref)}/q^2$. Here, the polymers in the simulations will be diluted without solvent molecules. As a result, the most crucial step in building the new simulations is to find the suitable bending potential so that the polymer chains have the size of $\langle R_0^2\rangle^*$. Because the newly designed systems have the same contour length, the target is to generate the same coil size under different concentrations. The corresponding values of the bending parameter κ are listed in Table 1. The new systems are labeled L100-nk2, L100-nk3, L100-nk4, and L100-nk6. When the system is diluted, the polymers will swell so that a smaller value of κ is needed compared to the standard density.

Figure 5 shows the comparison of the extensional viscosities between the reference systems and the newly designed systems.

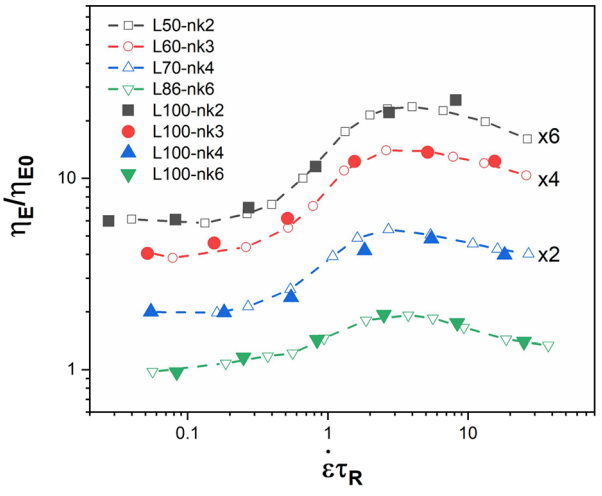

Figure 5. Normalized steady-state extensional viscosities of the simulations designed to test the Kuhn-scale criterion in eq 18. For clarity, the data with the reduced Kuhn density $n_k \approx 2$, 3, and 4 are vertically shifted by a factor of 6, 4 and 2, respectively.

The data are vertically adjusted for clarity. In Figure 2, it has been shown that the simulation systems have the same LVE property when they are unentangled. However, Figure 3 reveals that the same value of N_k cannot guarantee the same extensional viscosity when the chemistry (chain rigidity) changes. Nevertheless, Figure 5 shows that when the new system is similar to the reference in both N_k and n_k, their normalized extensional

https://doi.org/10.1021/acs.macromol.3c02648
Macromolecules 2024, 57, 5520−5532

viscosities agree quantitatively, even if there is a nontrivial entanglement effect. This means that the extensional rheology of the CG MD simulations indeed follows the universal feature suggested by eq 18. Thus, each pair of simulations can be considered as rheologically analogous liquids in both linear and nonlinear rheology. Furthermore, from the properties of these samples listed in Table 1, we can observe that neither the Kuhn length nor the packing length alone can explain why their extensional viscosities are so similar. Only their ratio, the reduced Kuhn density n_k, can account for it. In Figure 5, the simulation data show that the agreement between L50-nk2 and L100-nk2 will fail when $\dot{\epsilon}\tau_R > 10$. Investigating a higher flow Weissenberg number of the L100-nk2 sample from our current simulation method is unreliable because its Rouse time is too small and a very fast flow rate is required. The bead density in the L100-nk2 sample is too small, which causes the polymer chains to be almost entirely separated from each other when they are highly elongated. Thus, it should no longer be regarded as a concentrated liquid. However, for the other pairs, the agreement holds even in the extensional thinning regime. Overall, the prediction from the Kuhn-scale criterion in eq 18 is quite satisfying for the CG MD simulations.

3.6. Potential Universal Extensional Rheology in the Current Experimental Data from the Literature. It is worth investigating if some existing experimental data indicate the validity of the Kuhn-scale criterion proposed in this work, although most of the samples were not prepared based on this criterion. First, we can go back to the comparison between the simulation and experiment by Matsumiya et al.[15] in Figure 3. We can see that the quantitative agreement between the simulation data of L70-nk4 ($n_k \approx 4.31$) and PtBS ($n_k \approx 4.73$) is very close to the prediction of eq 18. As confirmed in the last section, the CG MD simulations have a unique extensional viscosity profile as long as the number of Kuhn segments and the reduced Kuhn density are fixed. This unique viscosity profile can also be observed in the experimental sample with the same Kuhn-scale properties in a nonlinear flow regime.

As explained in Section 1, the segmental details will unavoidably become non-negligible at some point. This means that the Kuhn-scale criterion will not work under arbitrarily fast flows for experimental samples. The comparison between the CG simulation and the unentangled PtBS in Figure 3 suggests that this happens when $\dot{\epsilon}\tau_R > 10$. In contrast, the extensional viscosity of the unentangled PS sample ($n_k \approx 4.54$),[17] which is expected to be similar to that of PtBS, suggests that the chemical structure of PS becomes a non-negligible factor when $\dot{\epsilon}\tau_R > 1$ with the molar mass of 27k. The difference in extensional viscosity between PS and PtBS may be due to the simpler chemical structure of styrene. As a result, it is easier to form some ordered structures under extension in PS than in PtBS, which cannot be accounted for in a CG chain model. This effect is especially prominent with a small molar mass of the sample. Under this interpretation, it is worth noting that the unentangled PS and PtBS samples measured by Matsumiya et al.[15] provide another valuable information. If we measure PS or PtBS with a higher molar mass, the impact of the chemical structure on the extensional viscosity will be observed under a much larger Rouse Weissenberg number. For example, $\dot{\epsilon}\tau_R = 1$ in PS of 27k means $\dot{\epsilon}\tau_R = 100$ in PS of 270k, far beyond the regime accessible by the current extensional rheometers. In fact, it has been reported by Morelly et al.[14] that the entangled melts of PS and PtBS have a very similar scaling in the extensional viscosity, which is consistent with the prediction of eq 18. The horizontal difference between the two sets of data could result from the difference in the number of Kuhn segments.

Another set of experimental data to discuss is the work by Sridhar et al.[60] This research showed that the extensional rheology of polymer melts and solutions has no fundamental difference when considering a wide range of chemical compositions. Additionally, the monotonic extensional-rate-thinning behavior observed in the entangled PS melt is not universal in polymer melts. The extensional viscosities of some other chemistries, such as polyisoprene (PI) and poly(n-butyl acrylate) (PnBA), can also show thickening after thinning in the melt state, just like the solution of PS. Therefore, the experimental data by Sridhar et al.[60] indicate the existence of an unrecognized parameter that can rationalize the extensional rheology of both melts and solutions. According to the Kuhn-scale criterion of eq 18 proposed in this work, we can understand the reasoning behind those data.[60] For example, the reduced Kuhn density value is 2.72 for PI (according to the plateau modulus used by Sridhar et al.,[60] the fraction of the 3−4 addition content in their material is around 7%), which is smaller than that of PS ($n_k \approx 4.54$).[17] This means that the melt of PI will be similar to a solution of PS with a weight fraction of 60% (ignoring the change of polymer size with concentration) in terms of their values of n_k and thus the two liquids will exhibit a comparable extensional viscosity based on the Kuhn-scale criterion of eq 18, as long as the molar mass is properly controlled. According to the previous experimental data,[10,11] the extensional viscosity of PS solution of this weight fraction will be nearly independent of the strain rate in the vicinity of $\dot{\epsilon}\tau_R = 1$, which is also observed in the PI melt by Sridhar et al.[60] This means that the prediction of eq 18 for PS and PI is valid, at least qualitatively. However, to justify this criterion quantitatively and systematically, which is an important task of our future studies, we will need to design and prepare the experimental samples very carefully.

At the same time, some experimental data do not align with the prediction of eq 18. For instance, the value of n_k is 4.07 for PMMA,[17] so we may expect a similar extensional viscosity of PMMA melt with the PS solution. This prediction contradicts the experimental data by Wingstrand et al.,[23] who reproduced the melt rheology of PS from the PMMA solution. However, it is important to note that in PS and PMMA, there is a significant violation of the Lin−Noolandi theory. According to eq 19, we would expect the number of Kuhn segments per entanglement N_{ek} of PMMA to be larger than that of PS by a factor of 1.24. However, the LVE data from the experiment show the opposite trend ($N_{ek} = 10$ for PMMA and $N_{ek} = 22$ for PS, as confirmed by Wingstrand et al.[23]). The disagreement with eq 19 can also be found in the series of poly(*n*-alkyl methacrylate) samples prepared by Wu et al.[16] The value of n_k for PHMA is larger than that of PMMA by a factor of 1.27,[17] but they have nearly the same N_{ek}. Indeed, while the Lin−Noolandi theory may be able to explain the overall trend in a broad range of chemistry, significant discrepancies could arise from the nontrivial prefactor α in eq 19 for a specific sample. This will be a completely different subject. However, all these facts must be seriously considered when searching for the potential universality in the nonlinear extensional rheology of experimental samples.

4. CONCLUSIONS

In this work, we quantitatively analyzed the interchain interaction in terms of the mean-field frictional coefficient in the CG MD simulations of unentangled polymer melts under

https://doi.org/10.1021/acs.macromol.3c02648
Macromolecules 2024, 57, 5520−5532

flow conditions. These frictional coefficients were found to be universally related to the projection areas of the polymer coil. This projection-friction relationship reveals that working on the Kuhn description of a concentrated polymeric liquid is sufficient to manipulate its nonlinear response to the fast flows. It also indicates a Kuhn-scale criterion of extensional viscosity, which means that similar extensional rheology will be observed when the samples have both the same number of Kuhn segments N_k and the same reduced density n_k, defined as the ratio of the Kuhn length and the packing length. Guided by this criterion, new simulation systems were designed to show similar LVE and extensional viscosity as a function of the reduced strain rate. In addition, specific experimental data in the literature have been discussed based on the proposed Kuhn-scale criterion. Consistent results were found when comparing the CG MD simulations with specific experimental data as well as from the comparison between experimental data of different chemistries. These findings can serve as a helpful guideline for the future experimental studies. To prove the existence of universal extensional rheology as indicated by our criterion, however, more systematic experimental works with careful sample preparation are still required.

This work also presents a challenging task for theoretical studies: explaining why the reduced Kuhn density is the crucial parameter in both linear and nonlinear dynamics. Even if the potential experimental data could validate the Kuhn-scale criterion of extensional viscosity, it remains an empirical criterion and is not proven by rigorous physical theories. Current results suggest that n_k seems to represent the fundamental element that will not be altered during the deformation of polymers. Despite the lack of a comprehensive understanding, we can hope that theoretical models could account for this Kuhn-scale property and further test this idea, in comparison to experimental data.

■ ASSOCIATED CONTENT

Supporting Information

The Supporting Information is available free of charge at https://pubs.acs.org/doi/10.1021/acs.macromol.3c02648.

Derivation of eq 8 from the Fokker−Planck equation of the bead−rod model and the justification of eqs 9 and 10 from the results of stochastic simulation (PDF)

■ AUTHOR INFORMATION

Corresponding Author

Nuofei Jiang − *Bio and Soft Matter, Institute on Condensed Matter and Nano-science, Université catholique de Louvain, 1348 Louvain-la-Neuve, Belgium;* orcid.org/0000-0002-6105-354X; Email: nuofei.jiang@uclouvain.be

Complete contact information is available at: https://pubs.acs.org/10.1021/acs.macromol.3c02648

Notes

The author declares no competing financial interest.

■ ACKNOWLEDGMENTS

I want to express my deep thanks to Prof. Evelyne van Ruymbeke for her generous help and consistent encouragement. I thank Prof. Hiroshi Watanabe for the helpful discussions, who patiently explained some fundamental concepts related to this work. I also thank Prof. Ravi Jagadeeshan and Dr. Isaac Pincus for the discussions on stochastic simulation. The thoughtful comments from the reviewers have been invaluable in refining the writing and strengthening the overall presentation. The support of the China Scholarship Council (CSC) - UCLouvain cofounding project is acknowledged. Computational resources have been provided by the Consortium des Équipements de Calcul Intensif (CÉCI), funded by the Fonds de la Recherche Scientifique de Belgique (F.R.S.-FNRS) under Grant No. 2.5020.11 and by the Walloon Region.

■ REFERENCES

(1) Doi, M.; Edwards, S. F. *The theory of polymer dynamics*; Oxford University Press: New York, 1986.

(2) Lin, Y. H. Number of entanglement strands per cubed tube diameter, a fundamental aspect of topological universality in polymer viscoelasticity. *Macromolecules* **1987**, *20* (12), 3080−3083.

(3) Kavassalis, T. A.; Noolandi, J. New View of Entanglements in Dense Polymer Systems. *Phys. Rev. Lett.* **1987**, *59* (23), 2674−2677.

(4) Fetters, L. J.; Lohse, D. J.; Richter, D.; Witten, T. A.; Zirkel, A. Connection between Polymer Molecular Weight, Density, Chain Dimensions, and Melt Viscoelastic Properties. *Macromolecules* **1994**, *27* (17), 4639−4647.

(5) Rouse, P. E. A theory of the linear viscoelastic properties of dilute solutions of coiling polymers. *J. Chem. Phys.* **1953**, *21* (7), 1272−1280.

(6) Tirtaatmadja, V.; Sridhar, T. A filament stretching device for measurement of extensional viscosity. *J. Rheol.* **1993**, *37* (6), 1081−1102.

(7) McKinley, G. H.; Sridhar, T. Filament-stretching rheometry of complex fluids. *Annu. Rev. Fluid Mech.* **2002**, *34*, 375−415.

(8) Bach, A.; Almdal, K.; Rasmussen, H. K.; Hassager, O. Elongational Viscosity of Narrow Molar Mass Distribution Polystyrene. *Macromolecules* **2003**, *36* (14), 5174−5179.

(9) Matsumiya, Y.; Watanabe, H. Non-Universal Features in Uniaxially Extensional Rheology of Linear Polymer Melts and Concentrated Solutions: A Review. *Prog. Polym. Sci.* **2021**, *112*, No. 101325.

(10) Huang, Q.; Mednova, O.; Rasmussen, H. K.; Alvarez, N. J.; Skov, A. L.; Almdal, K.; Hassager, O. Concentrated Polymer Solutions are Different from Melts: Role of Entanglement Molecular Weight. *Macromolecules* **2013**, *46* (12), 5026−5035.

(11) Huang, Q.; Alvarez, N. J.; Matsumiya, Y.; Rasmussen, H. K.; Watanabe, H.; Hassager, O. Extensional Rheology of Entangled Polystyrene Solutions Suggests Importance of Nematic Interactions. *ACS Macro Lett.* **2013**, *2* (8), 741−744.

(12) Huang, Q.; Hengeller, L.; Alvarez, N. J.; Hassager, O. Bridging the Gap between Polymer Melts and Solutions in Extensional Rheology. *Macromolecules* **2015**, *48* (12), 4158−4163.

(13) Costanzo, S.; Huang, Q.; Ianniruberto, G.; Marrucci, G.; Hassager, O.; Vlassopoulos, D. Shear and Extensional Rheology of Polystyrene Melts and Solutions with the Same Number of Entanglements. *Macromolecules* **2016**, *49* (10), 3925−3935.

(14) Morelly, S. L.; Palmese, L.; Watanabe, H.; Alvarez, N. J. Effect of Finite Extensibility on Nonlinear Extensional Rheology of Polymer Melts. *Macromolecules* **2019**, *52* (3), 915−922.

(15) Matsumiya, Y.; Watanabe, H.; Masubuchi, Y.; Huang, Q.; Hassager, O. Nonlinear Elongational Rheology of Unentangled Polystyrene and Poly(p-tert-butylstyrene) Melts. *Macromolecules* **2018**, *51* (23), 9710−9729.

(16) Wu, S.; Yang, H.; Chen, Q. Nonlinear Extensional Rheology of Poly(*n*-alkyl methacrylate) Melts with a Fixed Number of Kuhn Segments and Entanglements per Chain. *ACS Macro Lett.* **2022**, *11* (4), 484−490.

(17) Fetters, L. J.; Lohse, D. J.; Colby, R. H. *Chain Dimensions and Entanglement Spacings*; Springer: New York, 2007; 447−454.

(18) Marrucci, G.; Ianniruberto, G. Interchain Pressure Effect in Extensional Flows of Entangled Polymer Melts. *Macromolecules* **2004**, *37* (10), 3934−3942.

(19) Wagner, M. H.; Kheirandish, S.; Hassager, O. Quantitative prediction of transient and steady-state elongational viscosity of nearly monodisperse polystyrene melts. *J. Rheol.* **2005**, *49* (6), 1317−1327.
(20) Ianniruberto, G.; Brasiello, A.; Marrucci, G. In Friction coefficient does not stay constant in nonlinear viscoelasticity, *Proc. 7th Annu. Eur. Rheol. Conf.* 2011, 61.
(21) Ianniruberto, G.; Brasiello, A.; Marrucci, G. Simulations of Fast Shear Flows of PS Oligomers Confirm Monomeric Friction Reduction in Fast Elongational Flows of Monodisperse PS Melts As Indicated by Rheooptical Data. *Macromolecules* **2012**, *45* (19), 8058−8066.
(22) Yaoita, T.; Isaki, T.; Masubuchi, Y.; Watanabe, H.; Ianniruberto, G.; Marrucci, G. Primitive Chain Network Simulation of Elongational Flows of Entangled Linear Chains: Stretch/Orientation-induced Reduction of Monomeric Friction. *Macromolecules* **2012**, *45* (6), 2773−2782.
(23) Wingstrand, S. L.; Alvarez, N. J.; Huang, Q.; Hassager, O. Linear and Nonlinear Universality in the Rheology of Polymer Melts and Solutions. *Phys. Rev. Lett.* **2015**, *115* (7), No. 078302, DOI: 10.1103/PhysRevLett.115.078302.
(24) Ianniruberto, G.; Brasiello, A.; Marrucci, G. Modeling Unentangled Polystyrene Melts in Fast Elongational Flows. *Macromolecules* **2019**, *52* (12), 4610−4616.
(25) Masubuchi, Y.; Matsumiya, Y.; Watanabe, H. Test of Orientation/Stretch-Induced Reduction of Friction via Primitive Chain Network Simulations for Polystyrene, Polyisoprene, and Poly(n-butyl acrylate). *Macromolecules* **2014**, *47* (19), 6768−6775.
(26) Wagner, M. H.; Narimissa, E.; Masubuchi, Y. Elongational viscosity of poly(propylene carbonate) melts: tube-based modelling and primitive chain network simulations. *Rheol. Acta* **2023**, *62* (1), 1−14.
(27) Ramos, J.; Vega, J. F.; Martinez-Salazar, J. Predicting experimental results for polyethylene by computer simulation. *Eur. Polym. J.* **2018**, *99*, 298−331.
(28) Gartner, T. E.; Jayaraman, A. Modeling and simulations of polymers: A roadmap. *Macromolecules* **2019**, *52* (3), 755−786.
(29) Kremer, K.; Grest, G. S. Dynamics of entangled linear polymer melts: A molecular-dynamics simulation. *J. Chem. Phys.* **1990**, *92* (8), 5057−5086.
(30) Everaers, R.; Karimi-Varzaneh, H. A.; Fleck, F.; Hojdis, N.; Svaneborg, C. Kremer−Grest Models for Commodity Polymer Melts: Linking Theory, Experiment, and Simulation at the Kuhn Scale. *Macromolecules* **2020**, *53* (6), 1901−1916.
(31) Svaneborg, C.; Everaers, R. Characteristic Time and Length Scales in Melts of Kremer−Grest Bead−Spring Polymers with Wormlike Bending Stiffness. *Macromolecules* **2020**, *53* (6), 1917−1941.
(32) O'Connor, T. C.; Alvarez, N. J.; Robbins, M. O. Relating Chain Conformations to Extensional Stress in Entangled Polymer Melts. *Phys. Rev. Lett.* **2018**, *121* (4), No. 047801.
(33) O'Connor, T. C.; Hopkins, A.; Robbins, M. O. Stress Relaxation in Highly Oriented Melts of Entangled Polymers. *Macromolecules* **2019**, *52* (22), 8540−8550.
(34) Jiang, N.; van Ruymbeke, E. Variation of Spring Stiffness, Monomeric Friction, and Brownian Intensity in the Simulation System of Unentangled Melt under Steady Flow. *Macromolecules* **2023**, *56* (8), 2911−2929.
(35) Watanabe, H.; Matsumiya, Y.; Sato, T. Revisiting Nonlinear Flow Behavior of Rouse Chain: Roles of FENE, Friction-Reduction, and Brownian Force Intensity Variation. *Macromolecules* **2021**, *54* (8), 3700−3715.
(36) Matsumiya, Y.; Sato, T.; Chen, Q.; Watanabe, H. Rheo-Dielectric Behavior of Unentangled Poly (butylene oxide) under Steady Shear: Preliminary Evaluation of Non-Equilibrium Parameters at the Onset of Nonlinearity. *Nihon Reoroji Gakkaishi* **2022**, *50* (5), 371−385.
(37) Sato, T.; Matsumiya, Y.; Watanabe, H. Rheo-Dielectrics and Diffusion of Type-A Rouse Chain under Fast Shear Flow: Method of Evaluation of Non-Equilibrium Parameters for FENE, Friction-Reduction, and Brownian Force Intensity Variation. *Nihon Reoroji Gakkaishi* **2022**, *50* (2), 253−268.
(38) Matsumiya, Y.; Sato, T.; Chen, Q.; Watanabe, H. Rouse Analysis of Nonlinear Rheology of Unentangled Polymer Melts under Fast Shear: Viscoelastic Response to Superposed Oscillatory Strain. *Macromolecules* **2023**, *56* (8), 2930−2938.
(39) Todd, B. D.; Daivis, P. J. *Nonequilibrium molecular dynamics: theory, algorithms and applications*; Cambridge University Press, 2017.
(40) Thompson, A. P.; Aktulga, H. M.; Berger, R.; Bolintineanu, D. S.; Brown, W. M.; Crozier, P. S.; in't Veld, P. J.; Kohlmeyer, A.; Moore, S. G.; Nguyen, T. D.; Shan, R.; Stevens, M. J.; Tranchida, J.; Trott, C.; Plimpton, S. J. LAMMPS - a flexible simulation tool for particle-based materials modeling at the atomic, meso, and continuum scales. *Comput. Phys. Commun.* **2022**, *271*, No. 108171.
(41) Lees, A. W.; Edwards, S. F. The computer study of transport processes under extreme conditions. *J. Phys. C: Solid State Phys.* **1972**, *5* (15), 1921.
(42) Dobson, M. Periodic boundary conditions for long-time nonequilibrium molecular dynamics simulations of incompressible flows. *J. Chem. Phys.* **2014**, *141* (18), 184103.
(43) Nicholson, D. A.; Rutledge, G. C. Molecular simulation of flow-enhanced nucleation in n-eicosane melts under steady shear and uniaxial extension. *J. Chem. Phys.* **2016**, *145* (24), 244903.
(44) Everaers, R.; Sukumaran, S. K.; Grest, G. S.; Svaneborg, C.; Sivasubramanian, A.; Kremer, K. Rheology and microscopic topology of entangled polymeric liquids. *Science* **2004**, *303* (5659), 823−826.
(45) Ramirez, J.; Sukumaran, S. K.; Vorselaars, B.; Likhtman, A. E. Efficient on the fly calculation of time correlation functions in computer simulations. *J. Chem. Phys.* **2010**, *133* (15), 154103 DOI: 10.1063/1.3491098.
(46) Tassieri, M.; Ramírez, J.; Karayiannis, N. C.; Sukumaran, S. K.; Masubuchi, Y. i-Rheo GT: Transforming from Time to Frequency Domain without Artifacts. *Macromolecules* **2018**, *51* (14), 5055−5068.
(47) Hsu, H. P.; Kremer, K. Detailed analysis of Rouse mode and dynamic scattering function of highly entangled polymer melts in equilibrium. *Eur. Phys. J.-Spec. Top.* **2017**, *226* (4), 693−703.
(48) Kalathi, J. T.; Kumar, S. K.; Rubinstein, M.; Grest, G. S. Rouse Mode Analysis of Chain Relaxation in Homopolymer Melts. *Macromolecules* **2014**, *47* (19), 6925−6931.
(49) Bird, R. B.; Armstrong, R. C.; Hassager, O. *Dynamics of polymeric liquids: Vol. 2-kinetic theory*; Wiley, 1987.
(50) Hassager, O.; Mortensen, K.; Bach, A.; Almdal, K.; Rasmussen, H. K.; Pyckhout-Hintzen, W. Stress and neutron scattering measurements on linear polymer melts undergoing steady elongational flow. *Rheol. Acta* **2012**, *51* (5), 385−394.
(51) Mortensen, K.; Borger, A. L.; Kirkensgaard, J. J. K.; Huang, Q.; Hassager, O.; Almdal, K. Small-Angle Neutron Scattering Study of the Structural Relaxation of Elongationally Oriented, Moderately Stretched Three-Arm Star Polymers. *Phys. Rev. Lett.* **2021**, *127* (17), No. 177801, DOI: 10.1103/PhysRevLett.127.177801.
(52) Ianniruberto, G.; Marrucci, G. Origin of Shear Thinning in Unentangled Polystyrene Melts. *Macromolecules* **2020**, *53* (4), 1338−1345.
(53) Chu, K.-S.; Moroi, D. Self-diffusion in nematic liquid crystals. *J. Phys. Colloques* **1975**, *36* (C1), C1−99−C1−101.
(54) Shahid, T.; Clasen, C.; Oosterlinck, F.; van Ruymbeke, E. Diluting Entangled Polymers Affects Transient Hardening but Not Their Steady Elongational Viscosity. *Macromolecules* **2019**, *52* (6), 2521−2530.
(55) Milner, S. T. Unified Entanglement Scaling for Flexible, Semiflexible, and Stiff Polymer Melts and Solutions. *Macromolecules* **2020**, *53* (4), 1314−1325.
(56) Rubinstein, M.; Colby, R. H. *Polymer physics*; Oxford university press: New York, 2003.
(57) De Gennes, P.-G. *Scaling concepts in polymer physics*; Cornell university press, 1979.
(58) Uchidaa, N.; Grest, G. S.; Everaers, R. Viscoelasticity and primitive path analysis of entangled polymer liquids: From F-actin to polyethylene. *J. Chem. Phys.* **2008**, *128* (4), No. 044902, DOI: 10.1063/1.2825597.

https://doi.org/10.1021/acs.macromol.3c02648
Macromolecules 2024, 57, 5520−5532

(59) Hoy, R. S.; Kröger, M. Unified Analytic Expressions for the Entanglement Length, Tube Diameter, and Plateau Modulus of Polymer Melts. *Phys. Rev. Lett.* **2020**, *124* (14), No. 147801, DOI: 10.1103/PhysRevLett.124.147801.
(60) Sridhar, T.; Acharya, M.; Nguyen, D. A.; Bhattacharjee, P. K. On the Extensional Rheology of Polymer Melts and Concentrated Solutions. *Macromolecules* **2014**, *47* (1), 379−386.

https://doi.org/10.1021/acs.macromol.3c02648
Macromolecules 2024, 57, 5520−5532